Anomalous Dissipation Mechanism and Hall Quantization Limit in Polycrystalline CVD Graphene

F. Lafont[1], R. Ribeiro-Palau[1], Z. Han[2], A. Cresti[3], A. Delvallée[1], A. W. Cummings[4], S. Roche[4,5], V. Bouchiat[2], S. Ducourtieux[1], F. Schopfer[1] and W. Poirier[1*]

[1] *LNE - Laboratoire National de Métrologie et d'Essais, 78197 Trappes, France*

[2] *Institut Néel, CNRS - Université Joseph Fourier - Grenoble INP, 38042 Grenoble, France*

[3] *IMEP-LAHC (UMR5130), Grenoble INP MINATEC, 38016 Grenoble, France*

[4] *ICN2 - Institut Català de Nanociència i Nanotecnologia, Campus UAB, 08193 Bellaterra, Spain and*

[5] *ICREA - Instituciò Catalana de Recerca i Estudis Avançats, 08010 Barcelona, Spain*

(Dated: May 27, 2014)

We report on the observation of strong backscattering of charge carriers in the quantum Hall regime of polycrystalline graphene grown by chemical vapor deposition, which alters the accuracy of the Hall resistance quantization. The temperature and magnetic field dependence of the longitudinal conductance exhibits unexpectedly smooth power law behaviors, which are incompatible with a description in terms of variable range hopping or thermal activation, but rather suggest the existence of extended or poorly localized states at energies between Landau levels. Such states could be caused by the high density of line defects (grain boundaries and wrinkles) that cross the Hall bars, as revealed by structural characterizations. Numerical calculations confirm that quasi-1D extended non-chiral states can form along such line defects and short-circuit the Hall bar chiral edge states.

PACS numbers: 73.43.-f, 72.80.Vp

One manifestation of the Dirac physics in graphene is a quantum Hall effect (QHE)[1, 2] with a sequence of Hall resistance plateaus at $R_{\rm H} = \pm R_{\rm K}/(4(n+1/2))$ ($n \geqslant 0$ and $R_{\rm K} \equiv h/e^2$) and an energy spectrum quantized in Landau levels (LLs) at energies $E_n = \pm v_{\rm F}\sqrt{2\hbar neB}$, with a $4eB/h$ degeneracy (valley and spin)[4]. The QHE at LLs filling factor $\nu = \pm 2$ is very robust and can even survive at room temperature[3]. This comes from an energy spacing $\Delta E(B) = 36\sqrt{B}$ meVT$^{-1/2}$ between the first two degenerated LLs, which is larger than in GaAs ($1.7B$ meVT^{-1}) for accessible DC magnetic fields. This opens the door for a 10^{-9}-accurate quantum resistance standard in graphene, surpassing the usual GaAs-based one, in operating at lower magnetic fields ($B < 4$ T), higher temperature ($T > 4$ K) and higher measurement current ($I > 100$ μA)[5]. As confirmed from first investigations in exfoliated graphene[7–9], achieving such a device requires the production of a large area graphene monolayer ($\sim 10\,000$ μm^2) of high carrier mobility $\mu > 10\,000$ cm^{2}V^{-1}s^{-1} (assuming that $\mu B \gg 1$ is the relevant quantization criterion[6]) at homogeneous low carrier density ($n_{\rm s} < 2\times10^{11}$cm^{-2}). The quantization of $R_{\rm H}$ was thereby measured with an uncertainty of 9×10^{-11} in a large 35×160 μm^2 sample made of epitaxial graphene, at 14 T and 0.3 K[10]. Growth based on chemical vapor deposition (CVD) appears to be a promising route to produce large-area graphene with high mobility[11] in which the QHE is now commonly observed. However, in a 7×7 mm^2 sample, $R_{\rm H}$ at $\nu = 2$ was found to deviate from $R_{\rm K}/2$ by more than 10^{-2}, while the longitudinal resistance per square reached $R_{\rm xx} = 200$ Ω[12], which is the mark of a high dissipation, still unexplained. In comparison, a GaAs-based quantum resistance standard satisfies $R_{\rm xx} < 100$ $\mu\Omega$. This highlights the need for exploration of the precise transport mechanisms at work in CVD graphene. In this paper, we investigate

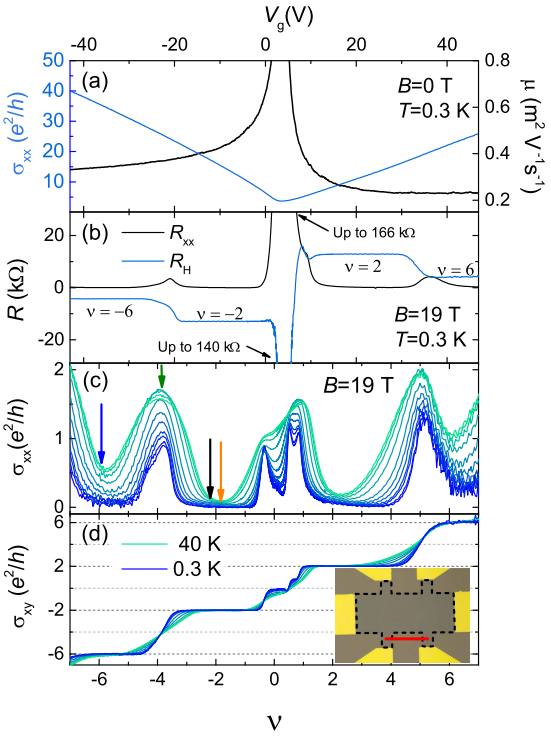

FIG. 1. a) Longitudinal conductance and deduced carrier mobility vs. V_g. b) $R_{\rm H}$ and $R_{\rm xx}$ vs. V_g. c) $\sigma_{\rm xx}$ and d) $\sigma_{\rm xy}$ vs. ν and V_g for T between 0.3 K and 40 K at 19 T. Insert of d): Hall bar optical image. The length scale (in red) between voltage terminals is 200 μm and equal to the Hall bar width.

the QHE in large Hall bars made of polycrystalline CVD graphene. We observe a strong dissipation characterized by an unexpected power law dependence of the conductance with T, B, and I which reveals an unconventional carrier backscattering mechanism. Structural characterizations bring out line defects crossing the devices, such as grain boundaries (GBs) or wrinkles naturally existing in polycrystalline CVD graphene. While some works exist at $B = 0$ T [35–39], the impact on transport of these line defects has been hardly investigated, to our knowledge, in the QHE regime[32–34]. With the support of numerical simulations we highlight their paramount role in limiting the Hall quantization.

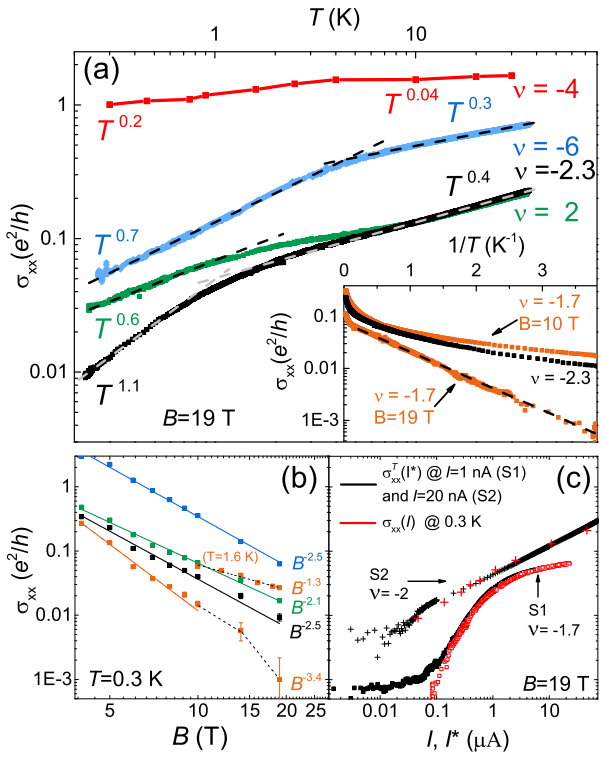

FIG. 2. a) σ_{xx} vs. T in log-log scale. Inset: σ_{xx} in log scale vs. $1/T$. b) σ_{xx} vs. B in log-log scale. c) σ_{xx} vs. I and σ_{xx}^{T} vs. I^* in log-log scale for two samples with $I^* = 0.87 \times T^{1.74}$ for S1 and $I^* = 0.6 \times T^{2.1}$ for S2.

Measurements were carried out with two large Hall bars (denoted S1 and S2) of 200×400 μm^2 size (inset of fig. 1d), patterned from polycrystalline CVD graphene grown on copper and then transferred to a SiO_2/Si substrate, see supplementary report[13]. Unless specified, presented results concern sample S1. Figure 1a shows the conductivity σ_{xx} as a function of the gate voltage V_g at 0.3 K and 0 T. The charge neutrality point (CNP) is positioned at $V_g = 3.5$ V, which indicates a residual hole density of 2.6×10^{11}cm^{-2}, assuming a SiO_2/Si back-gate efficiency of 7×10^{10} cm^{-2}/V. At large carrier density (1×10^{12}cm^{-2}), the hole (electron) mobility is ~ 3100 cm^{2}V^{-1}s^{-1} (~ 2300 cm^{2}V^{-1}s^{-1}). The electron phase coherence length L_ϕ, the inter-valley scattering length L_{iv}, and the intra-valley scattering length are 1.2 μm, 0.42 μm and 0.065 μm, respectively, as deduced from the measurement of the weak localization correction to the conductivity at 0.3 K[14]. The lower value of L_{iv} compared to L_ϕ indicates the presence of a significant concentration of short-range scatterers.

R_H, measured at 0.3 K and 19 T, is reported as a function of V_g and $\nu = n_s h/(eB)$ in fig. 1b. It features well-developed R_H plateaus at values $h/\nu e^2$ for $\nu = \pm 2, \pm 6$, which coincide with the minima of R_{xx}. Close to the CNP, additional high resistance peaks with $R_H, R_{xx} \gg h/e^2$ are observed, corresponding to plateaus marked by the transverse conductivity $\sigma_{xy} = R_H/(R_H^2 + R_{xx}^2)$ at 0 and e^2/h in fig. 1d. These plateaus are accompanied by minima of the longitudinal conductivity per square $\sigma_{xx} = R_{xx}/(R_H^2 + R_{xx}^2)$ also located around $\nu = 0$ and $\nu = 1$, respectively. Such conductivity plateaus can be explained by the degeneracy lifting of the n=0 LL[4, 15], which is usually observed in graphene with much higher carrier mobility. We therefore do not exclude the possibility that μ inside a monocrystalline grain would be higher than the moderate value calculated from the mean conductivity averaged over several grains. More extensive analysis of this observation is beyond the scope of this article.

Although nice plateaus are observed, it turns out that R_H is not well quantized, even on the $\nu = -2$ plateau, deviating from $R_K/2$ by more than 10^{-2} at a current of 1 μA, while R_{xx}, which reflects the dissipation arising from backscattering between counter-propagating quantum Hall edge states, is higher than 150 Ω. This is unexpected since the quantization of R_H has been measured with uncertainties several orders of magnitude lower in exfoliated graphene samples that are smaller than ours with similar carrier mobility[8, 9]. This shows that the transport properties in the QHE regime are very sensitive to the defect-type and that the mobility at $B = 0$ does not constitute a sufficient criteria of quantization in polycrystalline CVD graphene.

To identify the mechanism responsible for this loss of quantization σ_{xx}, which measures the dissipation level known as the quantization parameter[16], was analysed over a large range of ν values, at several temperatures between 0.3 K and 40 K (see fig. 1c), and at magnetic fields between 5 T and 19 T. Measurements of R_H and R_{xx} were carried out using a low-frequency AC measurement current of 1 nA, which ensures an absence of current effects (fig. 2c). Except for $\nu = -1.7$, where σ_{xx} reaches its minimum, and at B=19 T, it appears for both type of carriers (electrons and holes) that neither $\sigma_{xx}(T)$ (fig. 2a) nor $\sigma_{xx}(B)$ (fig. 2b) has an exponential behavior, which would be expected for a dissipation mechanism based on thermal activation to a higher-energy LL or variable range hopping (VRH) through lo-

calized states in the bulk. This greatly differs from what has been observed both in exfoliated[17–19] and epitaxial graphene[20]. Rather, whatever the quantum Hall state at $\nu = \pm 2, \ \pm 6$, σ_{xx} follows a power law dependence as a function of temperature ($\sigma_{xx} \propto T^{\alpha}$) and magnetic induction ($\sigma_{xx} \propto B^{-\beta}$) with $\alpha \in [0.3, 1.1]$ (at 19 T) and $\beta \in [2.1, 3.4]$ (at 0.3 K). The temperature dependence becomes smoother with ν moving away from the conductivity minimum. For $\sigma_{xx}(T)$, we can also define two temperature regimes characterized by larger α at lower temperature and a smooth crossover. In a given temperature regime and magnetic field, α slightly varies with ν, away from the LL centers. The same temperature behavior of σ_{xx}, with similar α values, was observed in sample S2, see supplementary report[13]. In S1, the dependence of σ_{xx} on T (B) becomes smoother with decreasing B (increasing T)(fig. 2a, 2b), characterized by decreasing values of α (β). Such behaviors are consistent with a reducing inter-LL energy gap. Interestingly, the σ_{xx} power law temperature dependence, observed for ν corresponding to σ_{xx} minima, is similar to that observed at σ_{xx} maxima, where charge transport is known to occur through extended LL states (as shown for $\nu = -4$ in fig. 2a). This suggests the scenario that the strong backscattering observed near $\nu = \pm 2, \pm 6$ is caused by extended or poorly localized states existing at energies between LLs.

At $\nu = -1.7$, a fit of $\sigma_{xx}(T)$ with an Arhenius law $\propto \exp(-(T_{act}/T))$ results in an activation temperature of 2.4 K $\ll \Delta E(B = 19\ \text{T})/k_B \sim 1834$ K, suggesting energy mobility edges unexpectedly far from the LL centers and confirming the fragility of the R_H quantization. A fit with a VRH theory including a soft Coulomb gap[21], $\propto (1/T)\exp(-(T_0/T)^{1/2})$, is also possible and leads to $T_0 = 27$ K and a high value for the localization length $\xi = Ce^2/(4\pi\epsilon_0\epsilon_r k_B T_0)$ (with $C \sim 6.2$[22]), equal to $\sim 1\ \mu\text{m} \gg l_B(19\ \text{T}) \sim 6$ nm [19, 23], which is the mark of poorly localized states in the bulk. Decreasing B from 19 T to 10 T, while ν is fixed at -1.7, results in a transition to a power law temperature dependence. This can be explained once again by the delocalization of states between LLs because of an increasing magnetic length $l_B = \sqrt{\hbar/(eB)}$, and increasing ξ, and a decreasing inter-LL energy gap.

The analysis of the dependence of σ_{xx} on the current is also instructive. Near $\nu = -2$, a significant increase of σ_{xx} starting from currents as low as 100 nA indicates a breakdown current density of the QHE lower than 5×10^{-3} A/m, which is unexpectedly small compared to values measured in epitaxial graphene (up to 43 A/m at 23 T)[24] or in exfoliated graphene (1 A/m)[8, 9]. This also suggests the existence of extended states accessible at low electric field. Moreover, fig. 2c shows that a similar current-temperature conversion relationship, $I^* \propto T^p$ with $p \sim 2$, exists for both samples S1 and S2, and regardless the exact temperature dependence of σ_{xx}. This allows for a good superposition of $\sigma_{xx}(I)$ and $\sigma^T_{xx}(I^*)$, where $\sigma_{xx}(T) = \sigma^T_{xx}(I^*)$, on a common current scale at sufficiently high I such that σ_{xx} is not limited by T. A relationship $I \propto T$ is expected in the QHE regime from the VRH mechanism[22], and was observed in exfoliated graphene[19]. On the other hand, $I \propto T^2$ was observed in graphene in the metallic regime, at low magnetic field[25] or in regime of Schubnikov-de-Haas oscillations[26] and explained by the coupling of carriers to acoustic phonons. This suggests that we can ascribe our observation of $I \propto T^2$ to the manifestation of metallic regime physics, which involves extended or poorly localized states, in a weakened QHE regime.

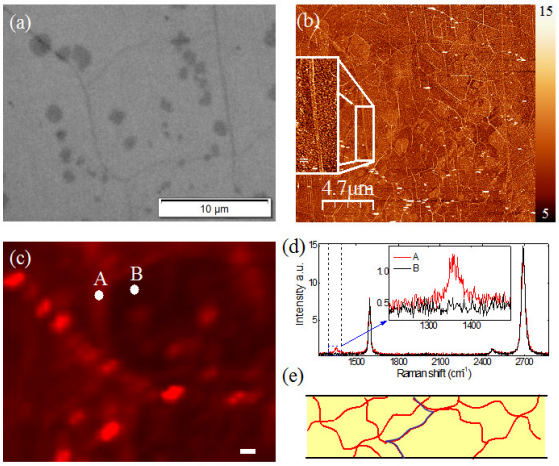

FIG. 3. a) Optical, b) AFM and c) Raman D peak (scale bar is 1.5 μm) pictures of about the same area of sample S2. d) Raman signal on (A) and away from (B) a wrinkle. e)Drawing of the a network of line defects corresponding to short-circuit paths between the sample edges.

To better understand our results, complementary structural analyses were performed combining different techniques (fig.3). Optical and atomic force microscopy reveal the existence of multilayer patches and a high density and variety of wrinkles. A multilayer patch is known to form mainly at the center of a grain during CVD growth[27], and from their spacing we can deduce typical monocrystalline grain sizes ranging from 1 μm to 10 μm (GBs were not directly observable with the techniques used). Given the small size of the patches (fig. 3a) compared to the width of the Hall bars and the ability of carriers to skirt local defects in the QHE regime[28], these patches are not expected to cause the observed strong backscattering. Raman spectroscopy in most of the optically clean areas indicate high quality graphene, since no D peak is observable (fig. 3c) [29]. On the other hand, the presence of the D peak, which confirms the existence of sharp defects, as already revealed by weak localization transport experiments, is measured at locations both on and away from wrinkles. Such a Raman D-peak is the signature of underlying defects such as va-

cancies or GBs[30, 31]. In our samples, wrinkles and GBs are likely to form a continuous network connecting Hall bar edges. Carriers moving from source to drain then cannot avoid crossing some line defects, which is expected to impact charge transport.

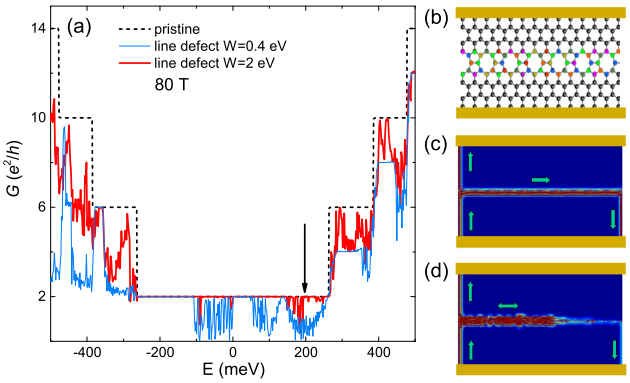

FIG. 4. a) Two-terminal magnetoconductivity of a pristine aGNR, and of aGNR with a 5-8 line defect crossing the sample (represented in b)) and including a random disorder potential. Spatial distribution of the electrons injected from the source contact (to the right) for W=0.4 eV c) and for W=2 eV d), at $E_F = 200$ meV. The arrows indicate the direction of the current flow. In particular, we can observe the chiral current along the edges and the more c) or less d) efficient short-circuit between the two.

To more closely study this impact on the QHE, we performed numerical calculations of the two-terminal conductivity of a 200 nm wide armchair graphene nanoribbon (aGNR) crossed by a line of pentagons and octagons[40, 41] by using the Green's function approach within the tight-binding framework[42]. To simulate a more realistic line defect, a random (Anderson[43]) potential with a uniform distribution in the range [-$W/2$,+$W/2$], where W is the disorder strength, was introduced on the line defect sites (fig. 4) to mimic a generic short-range disorder, as the one generated by ad-atoms or vacancies. In the QHE regime, the calculations reported were performed at B=80 T so that $l_B \sim 3$ nm is significantly smaller than the ribbon width (in a similar ratio of the experimental l_B to the smallest grain size) and larger than the interatomic distance. For a 100 nm-wide ribbon and B=40 T qualitatively very similar results, not shown, were obtained. The calculated conductivity almost systematically deviates from the value expected for pristine graphene by up to one spin-degenerated conduction channel, for weak disorder (0.4 eV) (fig.4), significantly larger than what is experimentally observed. The deviation is higher for electrons than for holes, where the asymmetry results from the sublattice symmetry breaking caused by the line defect. As demonstrated in fig. 4c, the deviation of the conductivity from the case of pristine graphene is caused by a circulating current along the line defect. An analysis of the energy spectrum shows that counter-propagating states on either side of the line defect can hybridize and form non-chiral quasi-1D extended states[44] able to carry current, which crosslink the opposite sample edges. Acting as a direct short-circuit, such states are responsible for a strong carrier backscattering. Remarkably, higher Anderson disorder reinforces wave-function localization along the line defect and reduces the circulation of current (fig. 4d), which finally improves the Hall conductivity quantization (fig. 4a). It is also found that, due to the disorder, the deviation of the Hall conductivity from pristine quantization reduces with increasing magnetic field and sample width (i.e. the length of the line defect network), both of which enhance the localization. See supplementary report for additional details[13]. Thus, a moderate alteration of the Hall conductivity quantization comparable to what is experimentally observed can be reproduced. Moreover, even though the simulations were run at 0 K, the existence of extended or poorly localized states along the line defect suggests smooth temperature behavior. Localization by strong disorder along the line defect also leads to the possible observation of VRH or thermal activation behavior, characteristic of an Anderson insulator. This is in sound agreement with our experimental observations, since, following the proposed scenario, σ_{xx} measured at ν values corresponding to minima should be dominated by the conductivity along the line defects, which is much higher than the bulk conductivity inside the grains. Finally, calculations performed for scrolled graphene[45] indicate that wrinkles are also expected to alter the Hall conductivity quantization in a similar fashion. Recent experimental results also suggest such an impact[34].

To conclude, in polycrystalline CVD graphene characterized by a high density of line defects such as GBs and wrinkles, we highlight unusual highly dissipative electronic transport in the QHE regime, which reveals the existence of poorly localized states between LLs and manifests itself as a deviation of R_H from the pristine quantization. Numerical simulations confirm that such states can exist along a line defect crossing a Hall bar and yielding strong backscattering between edge states. Further theoretical work, possibly considering Coulomb interactions and Luttinger physics[46], is required to explain the observed temperature, magnetic field and current dependence of σ_{xx}. Our work also motivates the investigation of the QHE in CVD graphene monocrystals, whose size is continuously in progress[47], not only to discern the respective roles of GBs and wrinkles but also to progress towards an operational graphene-based quantum resistance standard. More generally, it shows that the QHE is an efficient tool to reveal line defects in 2D materials, the precise characterization of which is crucial in view of future applications.

We wish to acknowledge D. Leprat and L. Serkovic for technical support, D. C. Glattli, J.-N. Fuchs, M. O.

Goerbig, S. Florens and Th. Champel for fruitful discussions. This research has received funding from the European Community's FP7, ERA-NET+, GraphOhm project (Grant No. 912/2009) and the French ANR, Metrograph project (Grant No. ANR-2011-NANO-004).

* wilfrid.poirier@lne.fr.

[1] K. S. Novoselov, A. K. Geim, S. V. Morozov, D. Jiang, M. I. Katsnelson, S. V. D. I. V. Grigorieva, and A. A. Firsov, Nature **438**, 197 (2005).
[2] Y. B. Zhang, Y. W. Tan, H. Stormer, and P. Kim, Nature **438**, 201 (2005).
[3] K. S. Novoselov, Z. Jiang, Y. Zhang, S. V. Morozov, H. L. Stormer, U. Zeitler, G. S. B. J. C. Maan, P. Kim, and A. K. Geim, Science **315**, 1379 (2007).
[4] M. O. Goerbig, Rev. Mod. Phys. **83**, 1193 (2011).
[5] W. Poirier and F. Schopfer, Nature Nanotechnology **5**, 171 (2010).
[6] F. Schopfer and W. Poirier, MRS bulletin **37**, 1255 (2012).
[7] A. J. M. Giesbers, G. Rietveld, E. Houtzager, U. Zeitler, R. Yang, K. S. Novoselov, A. K. Geim, and J. C. Maan, Appl. Phys. Lett. **93**, 222109 (2009).
[8] J. Guignard, D. Leprat, D. C. Glattli, F. Schopfer, and W. Poirier, Phys. Rev. B **85**, 165420 (2012).
[9] M. Wosczczyna, M. Friedemann, M. Gotz, E. Pesel, K. Pierz, T. Weimann, and F. J. Ahlers, Appl. Phys. Lett. **100**, 164106 (2012).
[10] T. J. B. M. Janssen, N. Fletcher, R. Goebel, J. Williams, A. Tzalenchuk, R. Yakimova, S. Kubatkin, S. Lara-Avila, and V. Falko, New J. Phys. **13**, 093026 (2011).
[11] N. Petrone, C. R. Dean, I. Meric, A. M. van der Zande, P. Y. Huang, L. Wang, D. Muller, K. L. Shepard, and J. Hone, Nano Lett. **12**, 2751 (2012).
[12] T. Shen, W. Wu, Q. Yu, C. A. Richter, R. Elmquist, D. Newell, and Y. P. Chen, Appl. Phys. Lett. **99**, 232110 (2011).
[13] Supplementary Report.
[14] E. McCann, K. Kechedzhi, V. I. Falko, H. Suzuura, T. Ando, and B. L. Altshuler, Phys. Rev. Lett. **97**, 146805 (2006).
[15] M. Kharitonov, Phys. Rev. B **85**, 155439 (2012).
[16] B. Jeckelmann and B. Jeanneret, Rep. Prog. Phys. **64**, 1603 (2001).
[17] A. J. M. Giesbers, U. Zeitler, M. I. Katsnelson, L. A. Ponomarenko, T. M. Mohiuddin, and J. C. Maan, Phys. Rev. Lett. **99**, 206803 (2007).
[18] A. J. M. Giesbers, U. Zeitler, L. A. Ponomarenko, R. Yang, K. S. Novoselov, A. K. Geim, and J. C. Maan, Phys. Rev. B **80**, 241411(R) (2009).
[19] K. Bennaceur, P. Jacques, F. Portier, P. Roche, and D. C. Glattli, Phys. Rev. B **86**, 085433 (2012).
[20] T. J. B. M. Janssen, A. Tzalenchuk, R. Yakimova, S. Kubatkin, S. Lara-Avila, S. Kopylov, and V. I. Falko, Phys. Rev. B **83**, 233402 (2011).
[21] B. I. Shklovskii and A. L. Efros, *Electronic properties of Doped semiconductors* (Springer, 1984).
[22] M. Furlan, Phys. Rev. B **57**, 14818 (1998).
[23] For $\xi >$ SiO_2 thickness, more accurate ξ estimation is expected from Mott-VRH..
[24] J. A. Alexander-Webber, A. M. R. Baker, T. J. B. M. Janssen, A. Tzalenchuk, S. Lara-Avila, S. Kubatkin, R. Yakimova, B. A. Piot, D. K. Maude, and R. J. Nicholas, Phys. Rev. Lett. **111**, 096601 (2013).
[25] A. M. R. Baker, J. A. Alexander-Webber, T. Altebaeumer, T. J. B. M. Janssen, A. Tzalenchuk, S. Lara-Avila, S. Kubatkin, R. Yakimova, C.-T. Lin, L.-J. Li, and R. J. Nicholas, Phys. Rev. B **86**, 235441 (2012).
[26] A. M. R. Baker, J. A. Alexander-Webber, T. Altebaeumer, S. D. McMullan, T. J. B. M. Janssen, A. Tzalenchuk, S. Lara-Avila, S. Kubatkin, R. Yakimova, C.-T. Lin, L.-J. Li, and R. J. Nicholas, Phys. Rev. B **87**, 045414 (2013).
[27] Z. Han, A. Kimouche, D. Kalita, A. Allain, H. Arjmandi-Tash, A. Reserbat-Plantey, L. Marty, S. Pairis, V. Reita, N. Bendiab, J. Coraux, and V. Bouchiat, Adv. Funct. Mater. **24**, 964 (2014).
[28] D. Yoshioka, *The quantum Hall effect* (Springer, 1998).
[29] A. C. Ferrari, Solid State Comm. **143**, 47 (2007).
[30] Q. Yu, L. A. Jauregui, W. Wu, R. Colby, J. Tian, Z. Su, H. Cao, Z. Liu, D. Pandey, D. Wei, T. F. Chung, P. Peng, N. P. Guisinger, E. A. Stach, J. Bao, S.-S. Pei, and Y. P. Chen, Nature Mat. **10**, 443 (2011).
[31] D. L. Duong, G. H. Han, S. M. Lee, F. Gunes, E. S. Kim, S. T. Kim, H. Kim, Q. H. Ta, K. P. So, S. J. Yoon, S. J. Chae, Y. W. Jo, M. H. Park, S. H. Chae, S. C. Lim, J. Y. Choi, and Y. H. Lee, Nature **490**, 235 (2012).
[32] L. Jauregui, H. Cao, W. Wu, Q. Yu, and Y. P. Chen, Solid State Comm. **151**, 1100 (2011).
[33] G.-X. Ni, Y. Zheng, S. Bae, H. R. Kim, A. Paschoud, Y. S. Kim, C.-L. Tan, J.-H. Ahn, B. H. Hong, and B. Ozyilmaz, ACSNano **6**, 1158 (2012).
[34] V. E. Calado, S.-E. Zhu, S. Goswami, Q. Xu, K. Watanabe, T. Taniguchi, G. C. A. M. Janssen, and L. M. K. Vandersypen, Appl. Phys. Lett. **104**, 023103 (2014).
[35] A. W. Tsen, L. Brown, M. Levendorf, F. Ghahari, P. Y. Huang, R. W. HAvener, C. S. Ruiz-Vargas, D. A. Muller, P. Kim, and J. Park, Science **336**, 1143 (2012).
[36] D. V. Tuan, J. Kotakoski, T. Louvet, F. Ortmann, J. Meyer, and S. Roche, Nano Lett. **13**, 1730 (2013).
[37] O. V. Yazyev and S. G. Louie, Nature Mat. **9**, 806 (2010).
[38] W. Zhu, T. Low, V. Perebeinos, A. A. Bol, Y. Zhu, H. Yan, J. Tersoff, and P. Avouris, Nano Lett. **12**, 3431 (2012).
[39] V. M. Pereira, A. H. Castro Neto, H. Y. Liang, and L. Mahadevan, Phys. Rev. Lett. **105**, 156603 (2010).
[40] D. A. Bahamon, A. L. C. Pereira, and P. A. Schulz, Phys. Rev. B. **83**, 155436 (2011).
[41] J. Song, H. Liu, H. Jiang, Q.-F. Sun, and X. C. Xie, Phys. Rev. B. **86**, 085437 (2012).
[42] A. Cresti, G. Grosso, and G. P. Parravicini, Eur. Phys. J. B **53**, 537 (2011).
[43] P. W. Anderson, Phys. Rev. **109**, 1492 (1958).
[44] A. W. Cummings, A. Cresti, and S. Roche, (unpublished).
[45] A. Cresti, M. M. Fogler, F. Guinea, A. H. Castro Neto, and S. Roche, Phys. Rev. Lett. **108**, 166602 (2012).
[46] M. P. A. Fisher and L. I. Glazman, in *Mesoscopic Electron Transport*, NATO ASI Series No. 345, edited by L. L. Sohn, L. P. Kouwenhoven, and G. Schon (Springer Netherlands, 1997) p. 331.
[47] H. Zhou, W. J. Yu, L. Liu, R. Cheng, Y. Chen, X. Huang, Y. Liu, Y. Wang, Y. Huang, and X. Duan, Nature Comm. **4**, 2096 (2013).